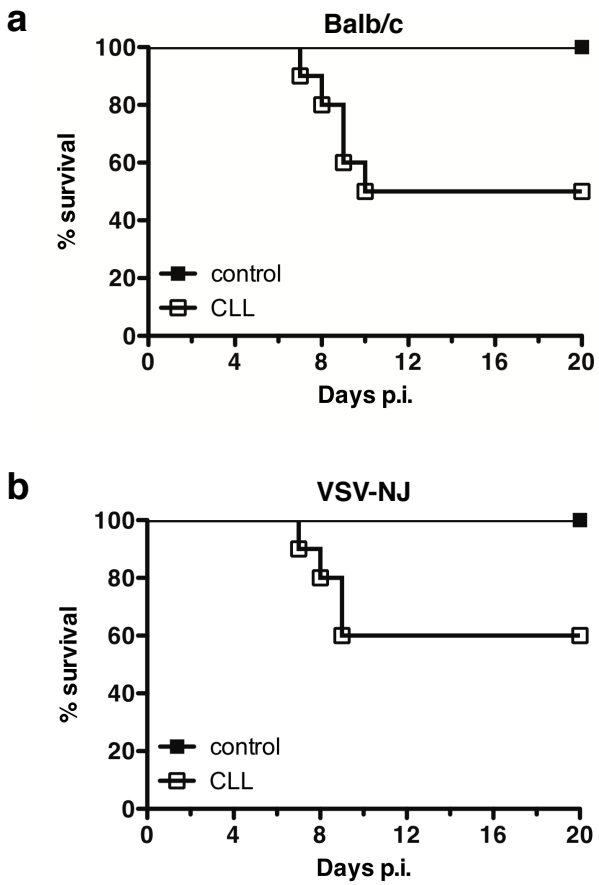

Supplementary Figure 1. *Lymph node macrophages confer resistance to lethal VSV infection regardless of the mouse strain or VSV strain used.* **a**, Kaplan-Meier survival curves of control or CLL-treated Balb/c mice after subcutaneous VSV Indiana infection. $n = 10$; $P < 0.0116$, Log-rank (Mantel-Cox) test. **b**, Kaplan-Meier survival curves of control or CLL-treated C57BL/6 mice after subcutaneous VSV New Jersey infection. $n = 10$; $P = 0.0295$**,** Log-rank (Mantel-Cox) test**.**

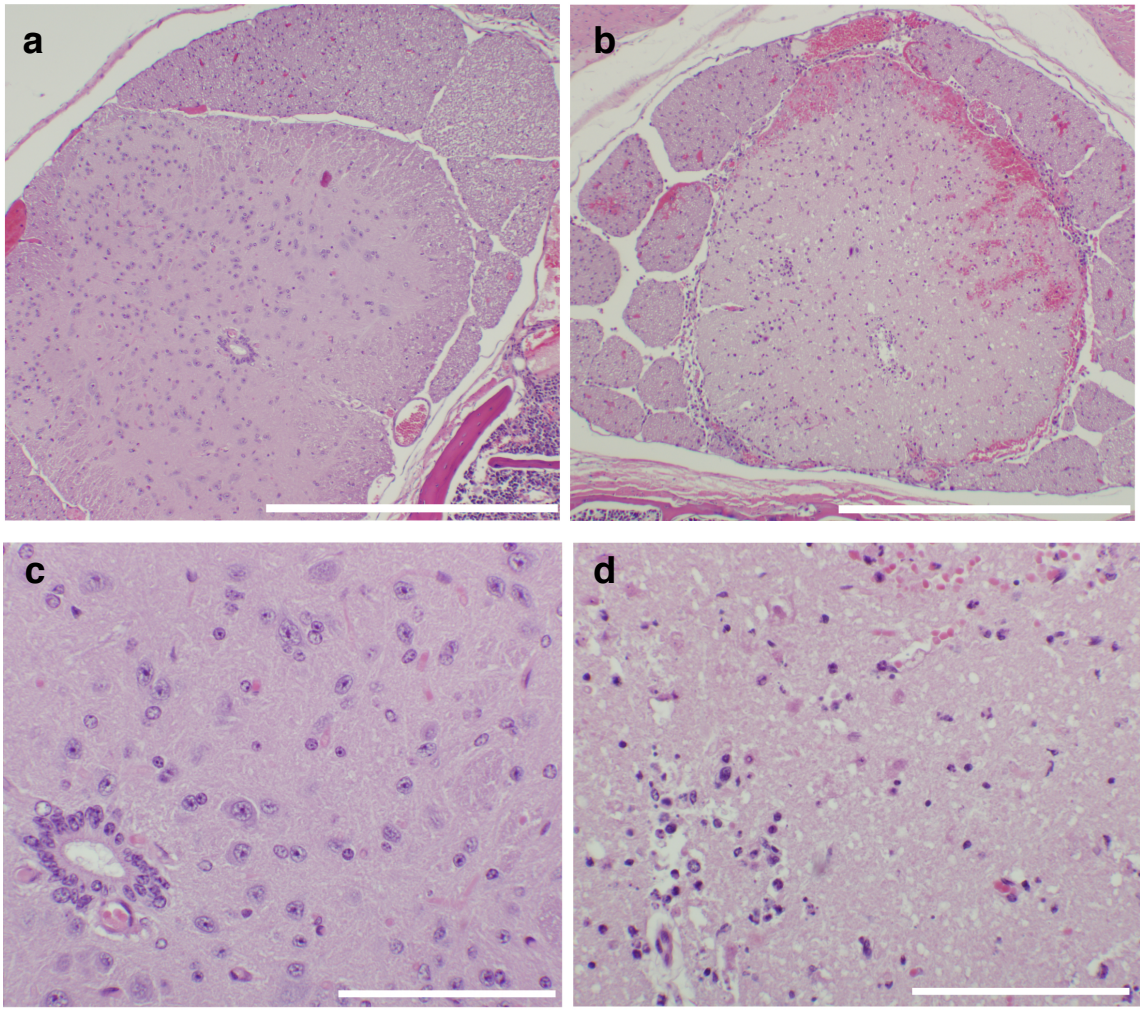

Supplementary Figure 2. *VSV-induced paralysis and death in macrophage-depleted animals is associated with extensive CNS pathology.* Micrographs of hematoxylin- and eosin-stained spinal cord cross sections from representative control (**a,c**) and symptomatic macrophage-depleted (**b,d**) mice, 7 days after sc VSV infection. Note that, while spinal cords and brains (not shown) from infected control mice were grossly normal (**a,c**), these same organs in symptomatic CLL-treated mice exhibited profound neuronal death, meningeal and parenchymal inflammatory infiltrate and diffuse hemorrhage (**b,d**). Images are representative of 3 mice/group. Scale bars reflect 500 μm (**a,b**) and 100 μm (**c,d**).

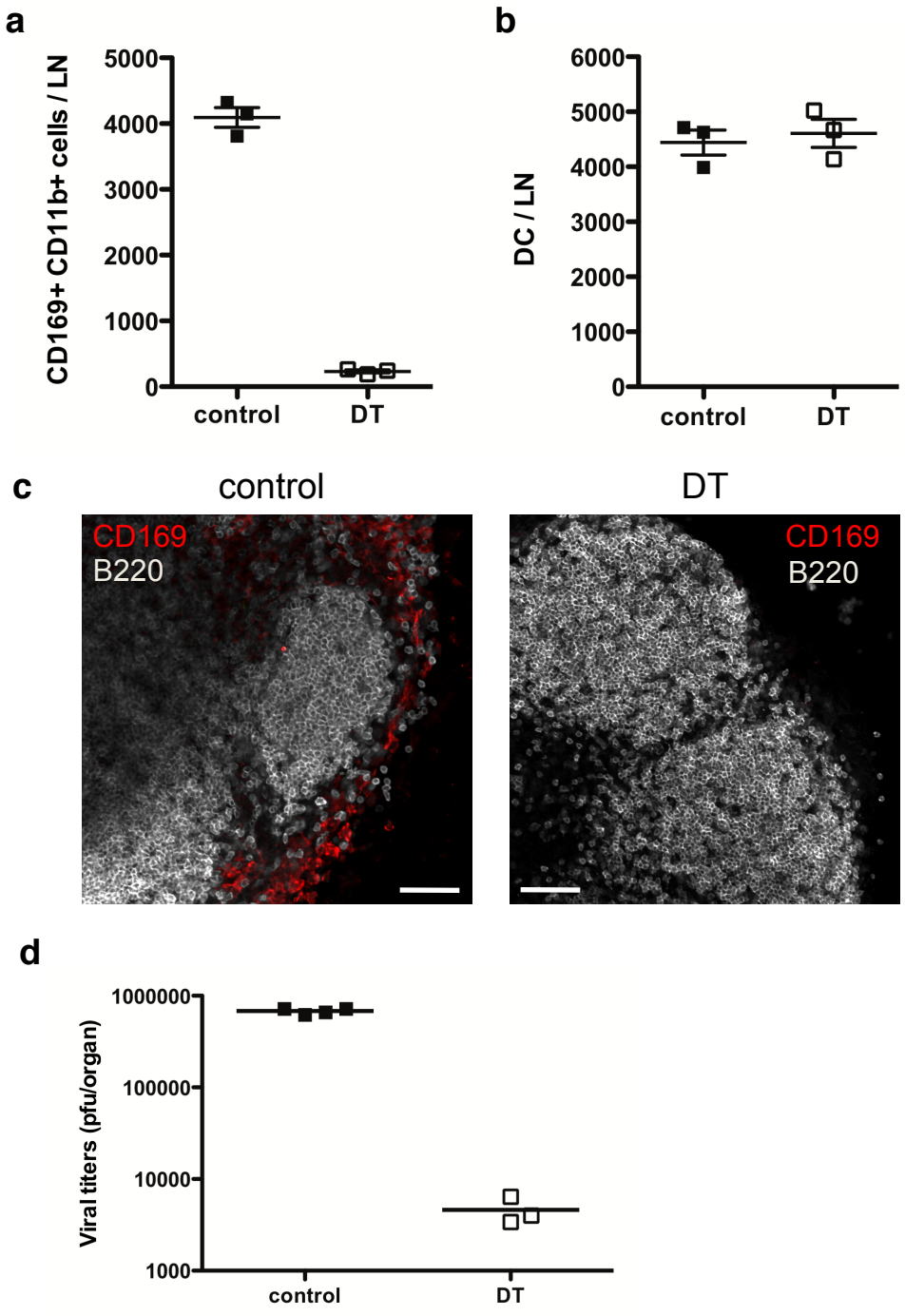

Supplementary Figure 3. *Diphtheria toxin treatment of CD11c-DTR mice selectively depletes CD169⁺ SCS macrophages*. **a**, CD169⁺ CD11b⁺ cell numbers in popliteal LNs of CD11c-DTR mice treated or not with diphtheria toxin (DT). $n = 3$, $P < 0.0001$. **b**, MHC-II^{hi} CD11c^{hi} cell numbers in popliteal LNs of CD11c-DTR mice treated or not with diphtheria toxin. $n = 3$, $P = 0.6516$. **c**, Representative confocal micrographs of popliteal LN sections from CD11c-DTR mice treated or not with diphtheria toxin. Anti-CD169 staining of macrophages in red, anti-B220 staining of B cells in white. Scale bar reflects 100 µm. **d**, Viral titers 30 min following subcutaneous injection of VSV (2 x 10^6 pfu / mouse) in popliteal LNs of CD11c-DTR mice treated or not with diphtheria toxin. $n = 4$ (control), $n = 3$ (DT), $P < 0.0001$.

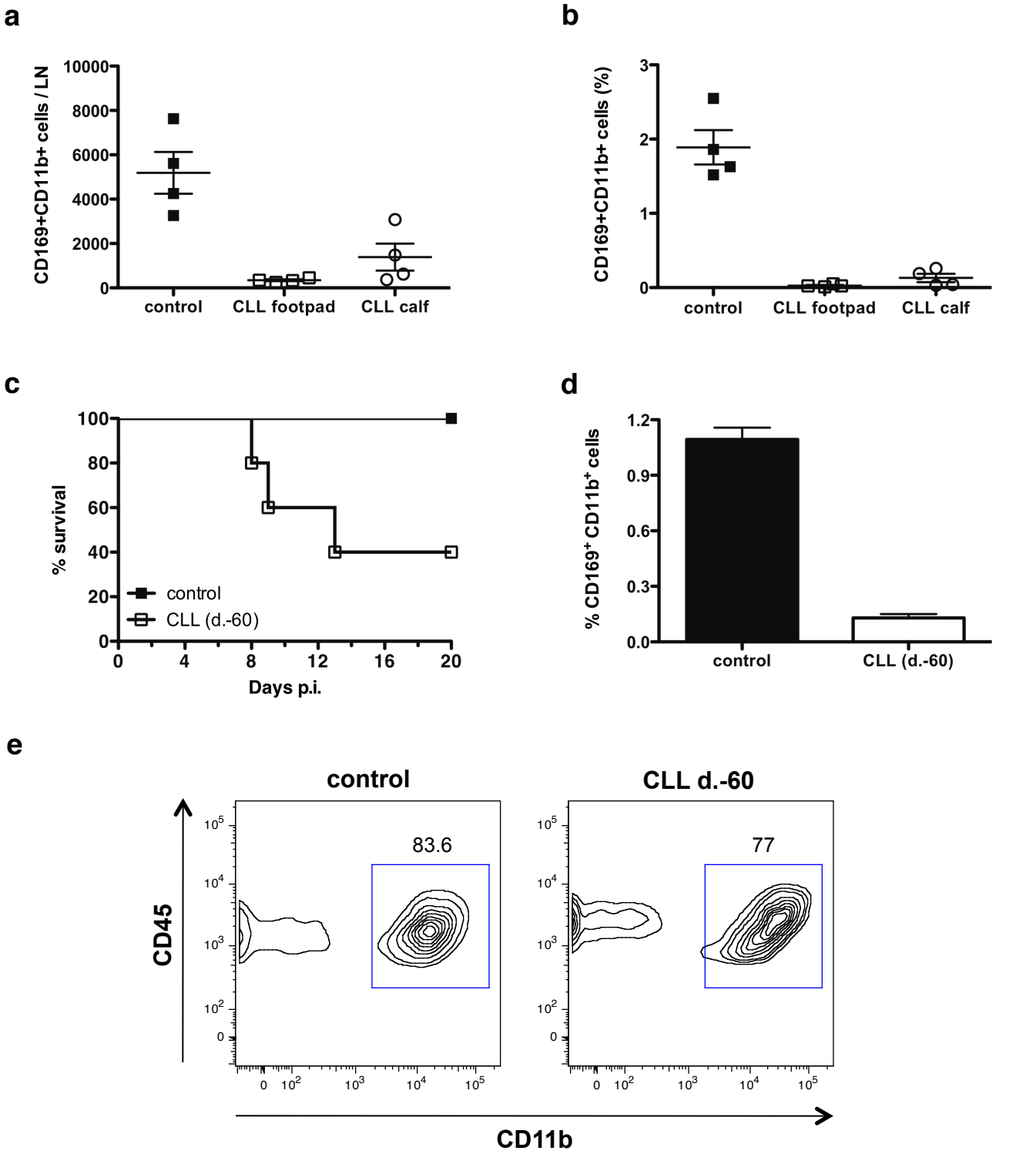
a
CD169+CD11b+ cells / LN
10000
8000
6000
4000
2000
0
control
CLL footpad
CLL calf
b
CD169+CD11b+ cells (%)
3
2
1
0
control
CLL footpad
CLL calf
c
% survival
100
80
60
40
20
0
control
CLL (d.-60)
0
4
8
12
16
20
Days p.i.
d
% CD169+ CD11b+ cells
1.2
0.9
0.6
0.3
0.0
control
CLL (d.-60)
e
control
CLL d.-60
CD45
83.6
77
CD11b

Supplementary Figure 4. *Injection of CLL in the calf depletes LN macrophages in the draining popliteal LN.* **a**, Quantification (percentage of total LN cells) of LN macrophages in popliteal LN single cell suspensions from control mice and mice injected sc with CLL in the footpad or calf. $n = 4$, all $P < 0.001$, except CLL footpad versus CLL calf, not significant. **b**, Quantification (absolute numbers) of LN macrophages in the mice treated as in **a**. $n = 4$, all $P < 0.01$, except CLL footpad versus CLL calf, not significant. Data in **a** and **b** are representative of 2 independent experiments. **c**, Kaplan-Meier survival curves following subcutaneous VSV infection of control mice or mice treated with footpad CLL 60 days prior to infection. $n = 5$, $P = 0.0494$, Log-rank (Mantel-Cox) test**. d**, Quantification (percentage of total LN cells) of LN macrophages in popliteal LN single cell suspensions from control mice and mice injected sc with CLL in the footpad 60 days prior to analysis. $n = 3$, $P < 0.0001$, *t*-test. **e**, FACS plots of single-cell suspensions from digested footpads of control mice (left) and mice injected sc with CLL 60 days prior to analysis (right). Numbers represent the percentage of $CD11b^+$ cells within $CD45^+$ cells. Plots are representative of 3 mice per group.

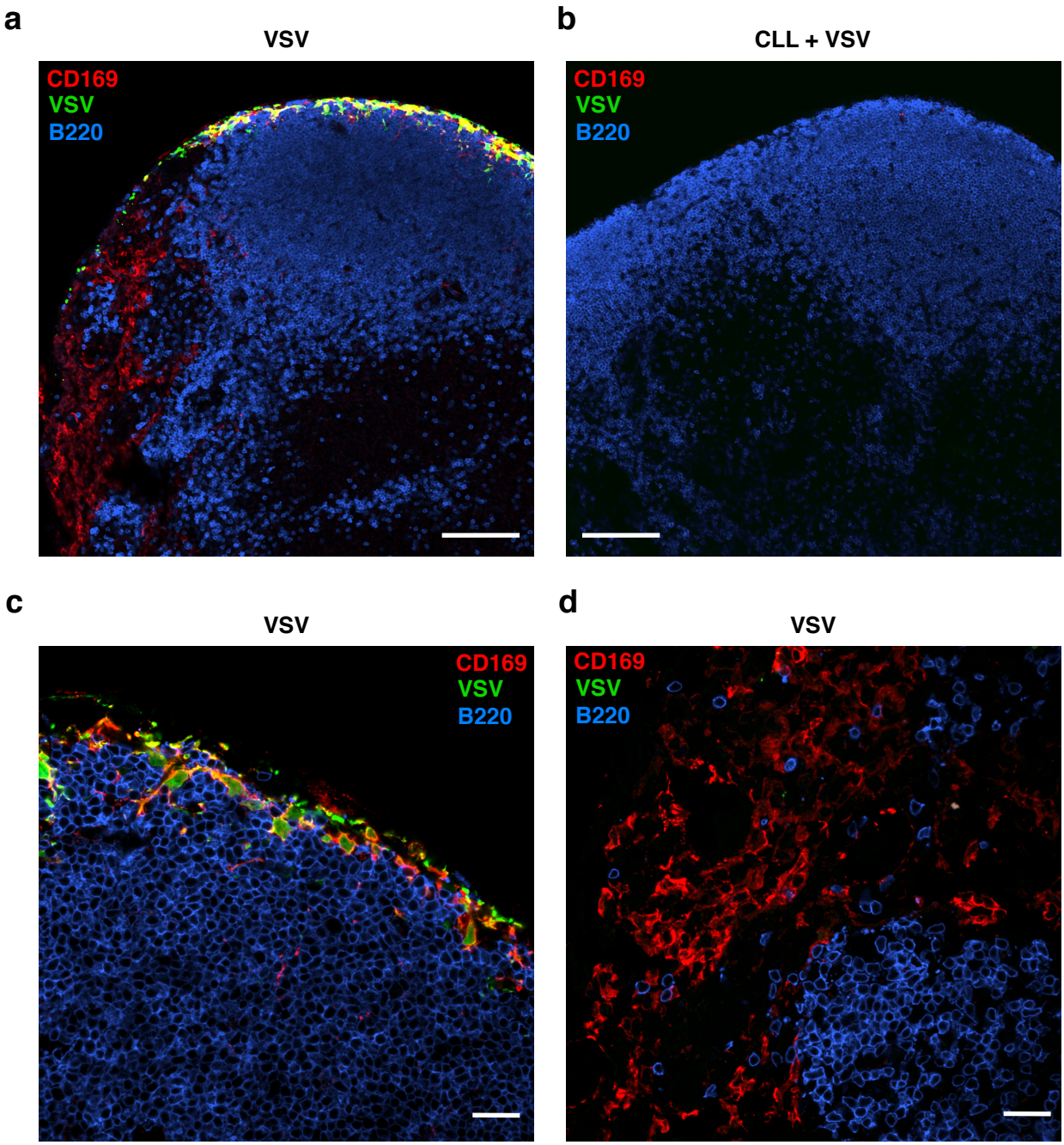

Supplementary Figure 5. *VSV replicates selectively in SCS macrophages and not in medullary macrophages.* **a,b,** Confocal micrographs of control popliteal LN (**a**) and CLL-treated popliteal LN (**b**) infected with VSV-eGFP (green) and stained in red with anti-CD169 for LN macrophages, and in blue with anti-B220 for B cells. **c**, Confocal micrograph of CD169+ SCS macrophages following subcutaneous VSV-eGFP infection. **d**, Confocal micrograph of CD169+ medullary macrophages following subcutaneous VSV-eGFP infection. All images are representative of 10 popliteal LNs, from 3 independent experiments. Scale bars reflect 100 μm (**a,b**) and 20 μm (**c**,**d**).

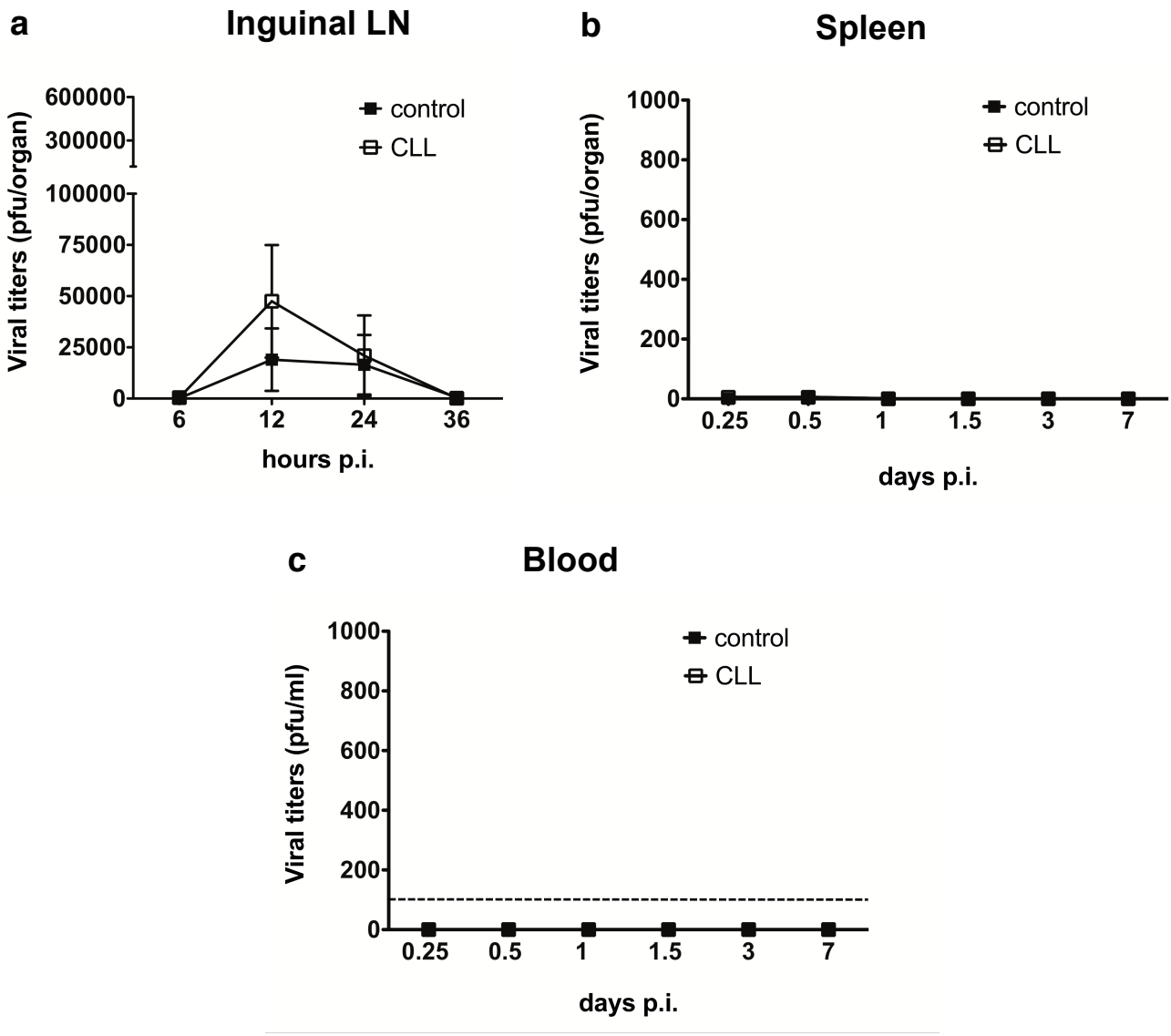

Supplementary Figure 6. *Viral titers in different organs of macrophage-depleted mice upon VSV infection.* Viral titers from inguinal LNs (**a**), spleens (**b**) and blood (**c**) of control mice and footpad CLL treated mice at the indicated time points following subcutaneous footpad VSV infection. Broken line indicates limit of detection. *n* = 6, differences were all non-significant. Data are representative of 2 independent experiments.

Suppl. Fig. 7

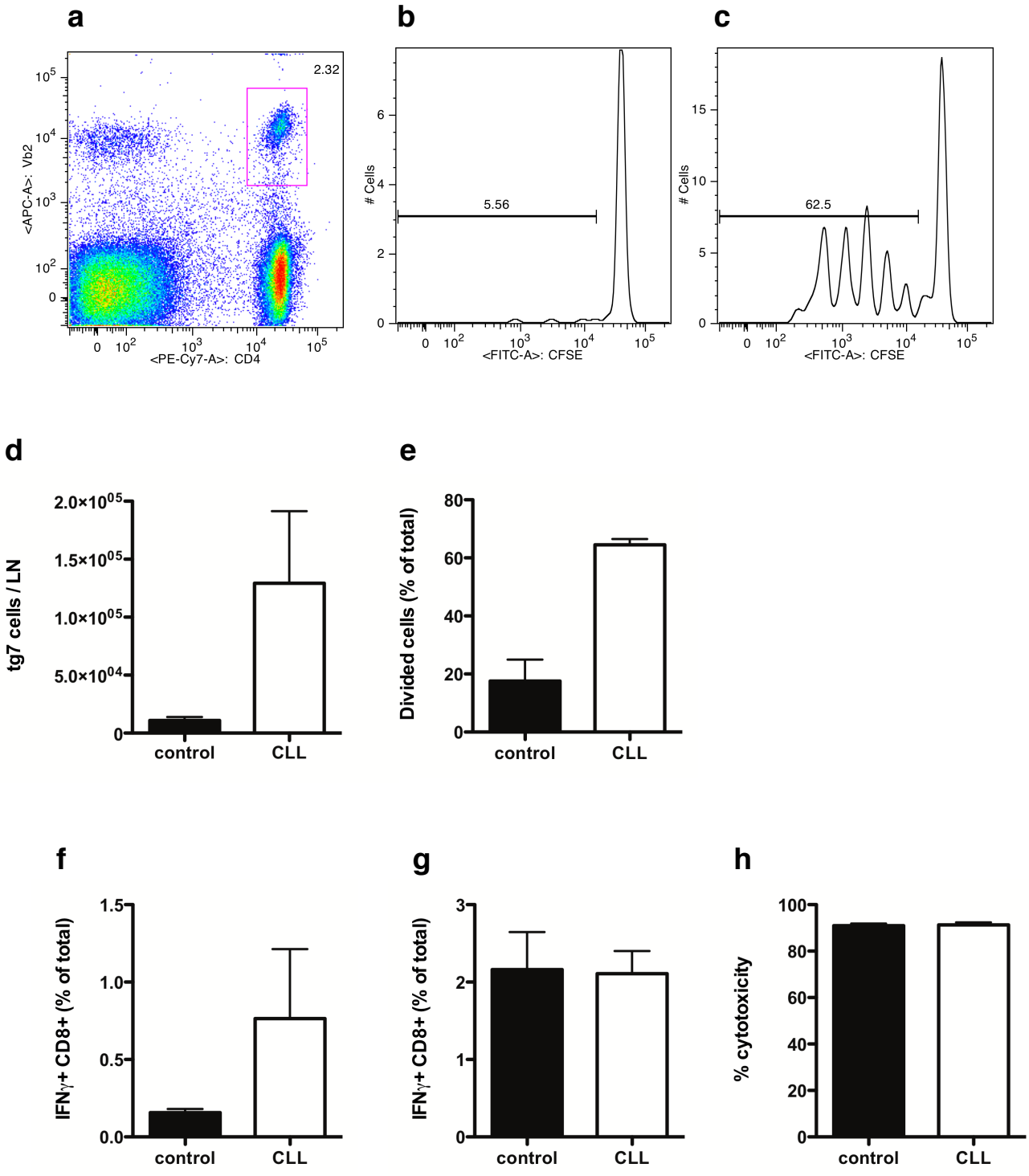
a
b
c
2.32
<APC-A>: Vb2
<PE-Cy7-A>: CD4
5.56
Cells
<FITC-A>: CFSE
62.5
d
e
tg7 cells / LN
Divided cells (% of total)
control
CLL
f
g
h
IFNγ+ CD8+ (% of total)
% cytotoxicity

Supplementary Figure 7. *T cell responses in macrophage-depleted mice upon VSV infection*. **a**, FACS plot illustrating gating strategy used to identify transferred VSV-specific CD4 TCR transgenic (tg7) cells in LNs of VSV infected mice. **b,c**, Representative CFSE dilution profile of tg7 CD4+ T cells 3 days after subcutaneous VSV infection of control mice (**b**) or CLL treated mice (**c**). $n = 3$. **d**, Quantification of total number of tg7 $CD4^+$ T cells in popliteal LNs of control and CLL treated LNs 3 days after footpad VSV infection. $n = 3$, $P = 0.1294$. **e**, Percentage of tg7 $CD4^+$ T cells that had undergone at least 1 division following footpad VSV infection in draining popliteal LN of control and CLL treated mice 3 days after infection. $n = 3$, $P = 0.0166$. **f**, Percentage of ex vivo IFNγ-producing $CD8^+$ T cells from control and CLL treated LNs 7 days after footpad VSV infection. $n = 4$, $P = 0.3047$. **g**, Percentage of IFNγ-producing $CD8^+$ T cells in LN cell suspensions from the same mice described in **f**, after 5 hour in vitro restimulation with N52-59. Differences were not significant. **h**, In vivo cytotoxicity assay (see Methods) in control or CLL-treated LNs 7 days after VSV infection. Differences were not significant.

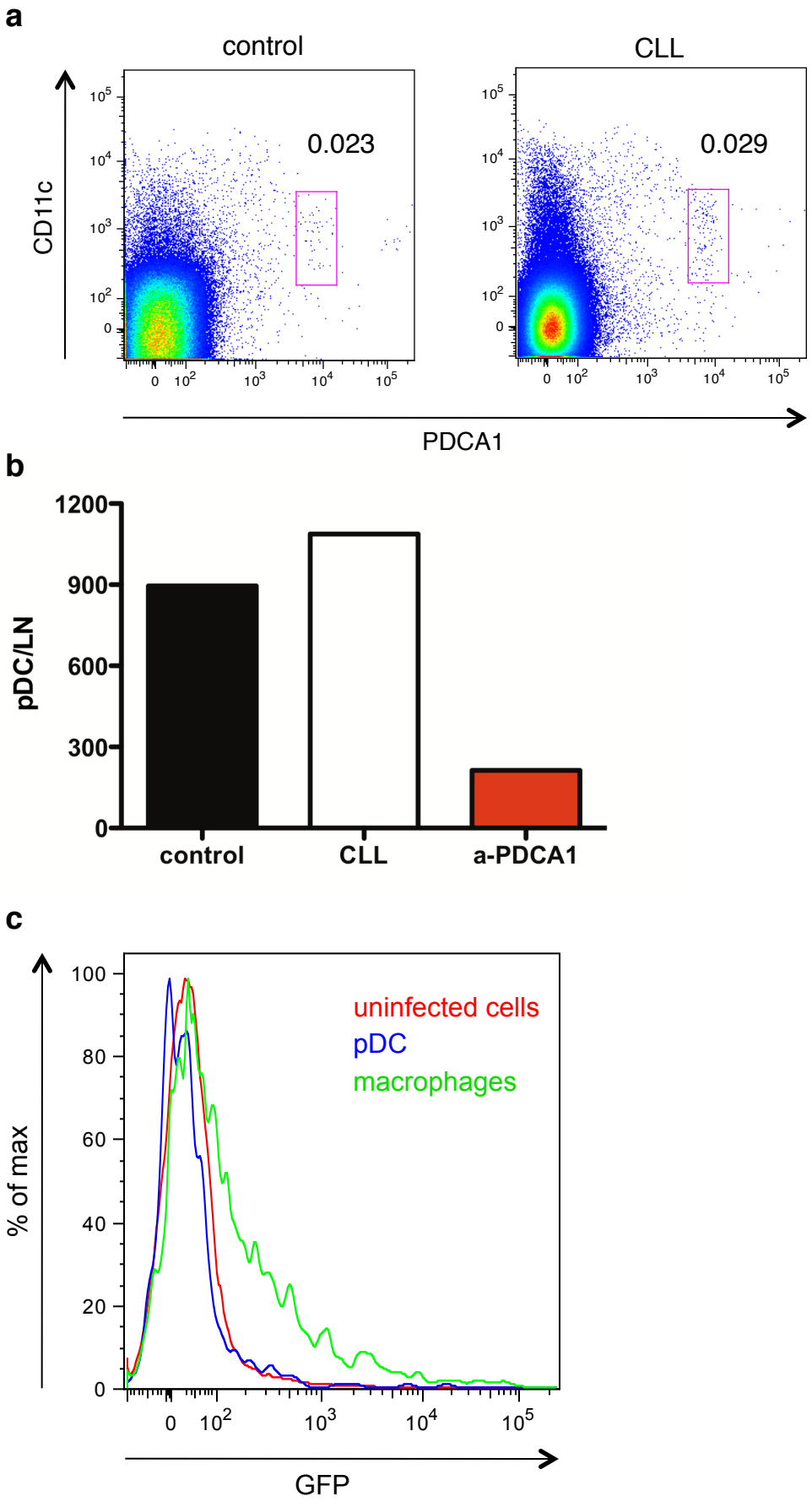
a
control
CLL
0.023
0.029
CD11c
PDCA1
b
pDC/LN
1200
900
600
300
0
control
CLL
a-PDCA1
c
% of max
100
80
60
40
20
0
uninfected cells
pDC
macrophages
GFP

Supplementary Figure 8. *Analysis of pDCs in popliteal LNs*. **a**, Representative FACS plots depicting pDC frequency in control and CLL-treated LN. The results are representative of 3 independent experiments that showed similar results. **b,** pDC numbers in popliteal LNs of control, CLL-treated, and a-PDCA1 treated animals. Results are representative of 3 independent experiments that showed similar results. **c,** FACS histogram plot showing the mean fluorescence intensity of the GFP signal in single cell suspensions from draining popliteal LN from mice that had been infected with VSV-eGFP 8 hours earlier. $CD169^+$ $CD11b^+$ macrophages in green, $CD11c^{int}$ $B220^+$ $Gr\text{-}1^+$ pDCs in blue and uninfected cells in red. The results are representative of 3 independent experiments that showed similar results.

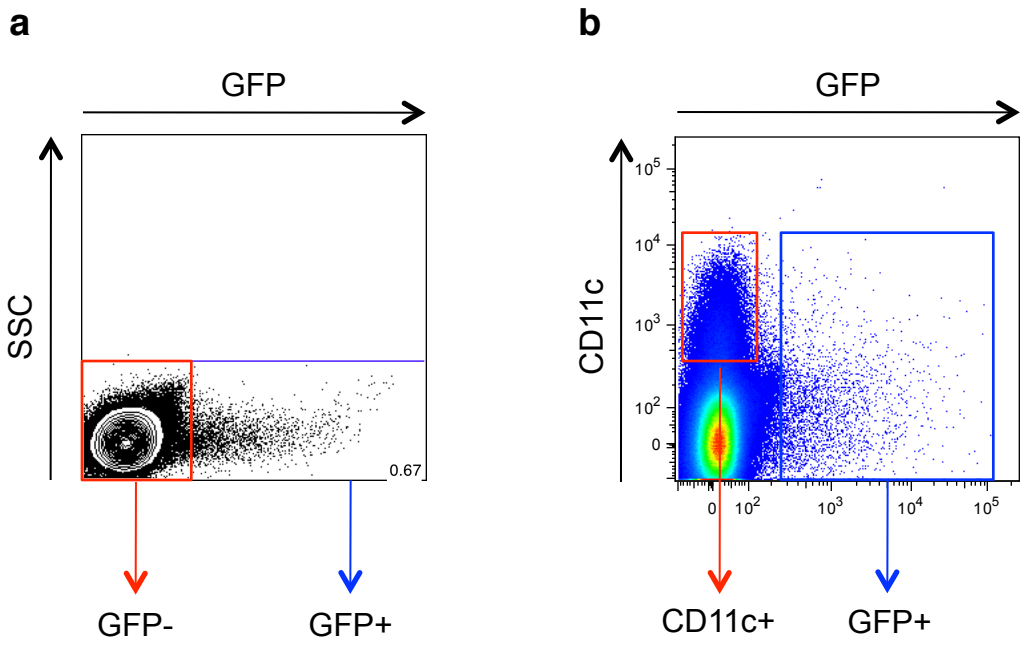

Supplementary Figure 9. *Sorting strategies used to analyze cell-specific IFN-I production*. **a,b**, FACS plot from single suspensions of LN cells 4 hours after subcutaneous VSV-eGFP infection depicting the sorting strategies used in the experiments described in Figure 3b (**a**) and Figure 3c (**b**).

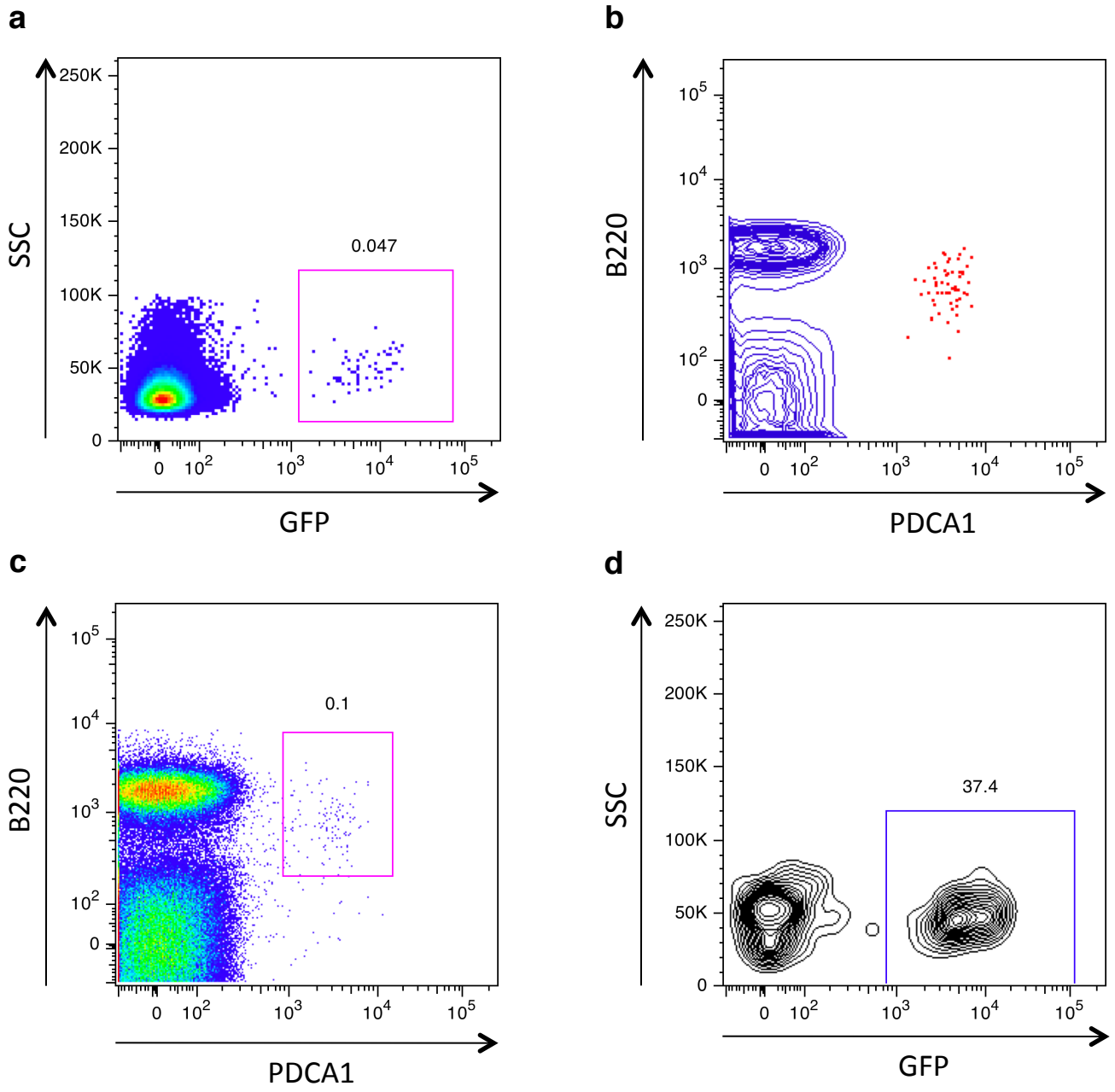

Supplementary Figure 10. *Characterization of DPE-GFP-RAG2$^{-/-}$:C57BL/6 mixed bone marrow chimeric mice*. **a**, FACS plot showing the characterization of GFP-expressing cells in DPE-GFP-RAG2$^{-/-}$:C57BL/6 mixed (30:70) bone marrow chimeric mice. **b**, FACS plot showing the expression of B220 and PDCA1 in the cells gated in **a** (red) or in the total single cell suspension from LNs of a DPE-GFP-RAG:C57BL/6 mixed (30:70) bone marrow chimeric mouse (blue). **c**, FACS plot showing the expression of B220 and PDCA1 in single cell suspension from LNs of a DPE-GFP-RAG:C57BL/6 mixed (30:70) bone marrow chimeric mouse. **d**, FACS plot of the cells gated in **c**, showing the relative expression of GFP. The results indicate that ~30% of pDCs in these mice express GFP. The FACS plots shown in **a-d** are representative of 3 independent experiments that showed similar results.

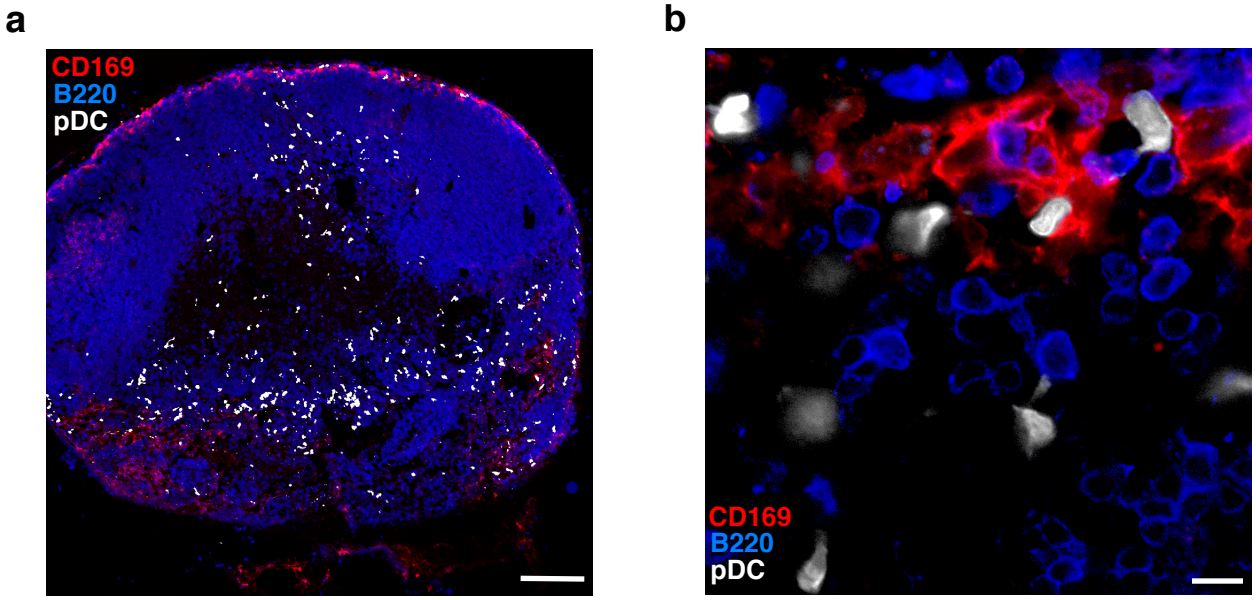

Supplementary Figure 11. *pDC relocalization and interaction with CD169+ macrophages within draining LN upon VSV infection*. **a,b**, Confocal micrographs of representative popliteal LN sections from irradiated C57BL/6 mice that were reconstituted with a 70:30 mixture of bone marrow from C57BL/6 and DPE-GFPxRAG2$^{-/-}$ donors and sacrificed 8h after VSV infection. Scale bars reflect 150 μm (**a**) or 8 μm (**b**). DPE-GFPxRAG2$^{-/-}$ pDC expressing GFP are shown in white; sections were counterstained with anti-CD169 (red) and anti-B220 (blue) to identify macrophages and B cells, respectively.

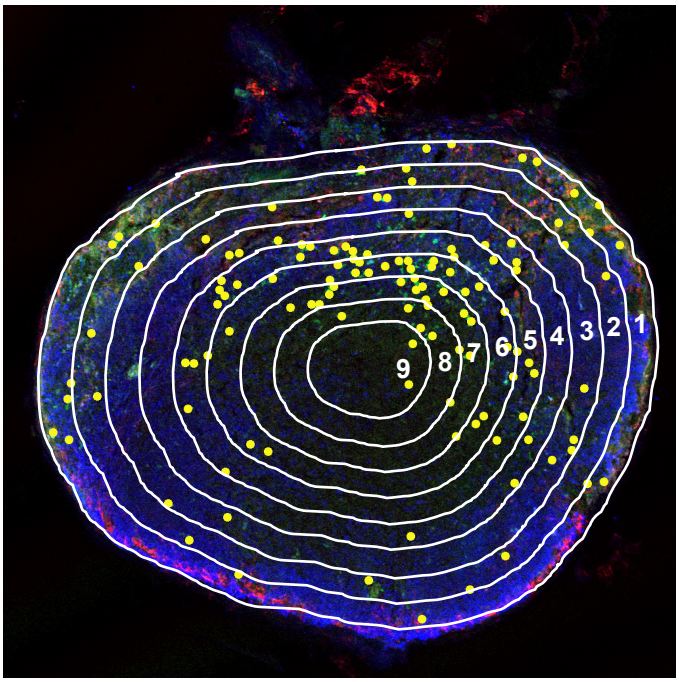

Supplementary Figure 12. *Methodology used to assess pDC frequency distribution relative to the LN capsule*. Representative confocal micrograph depicting the strategy used to assess pDC frequency distribution in Fig. 3i. A perimeter was drawn around each LN section and subsequently resized by 10% reductions. The number of pDCs that were located in each concentric ring was counted and plotted as frequency distribution.

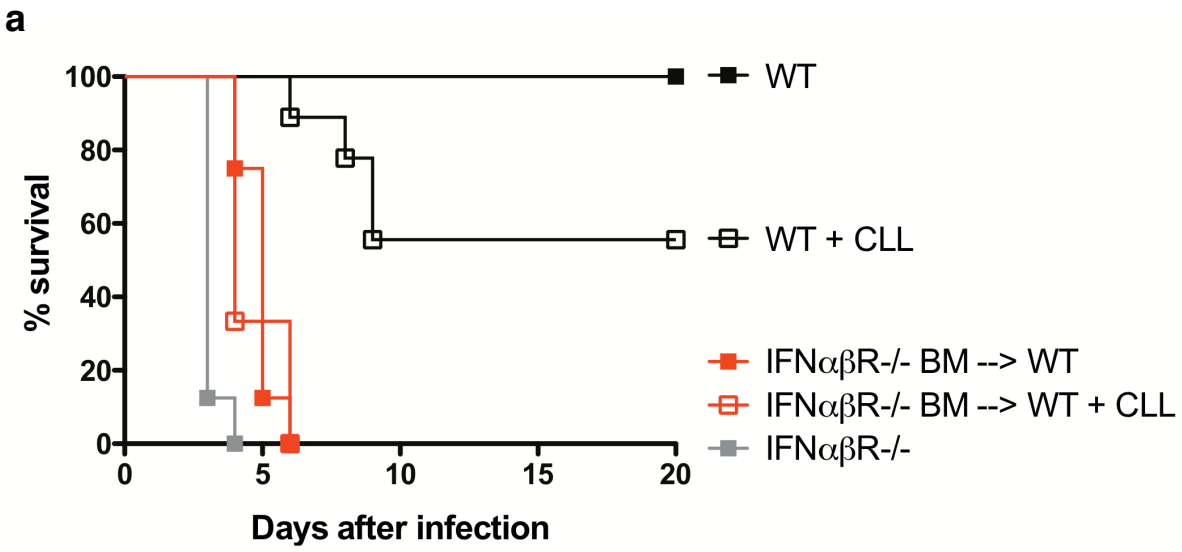
a
100
80
60
40
20
0
% survival
0
5
10
15
20
Days after infection
WT
WT + CLL
IFNαβR-/- BM --> WT
IFNαβR-/- BM --> WT + CLL
IFNαβR-/-

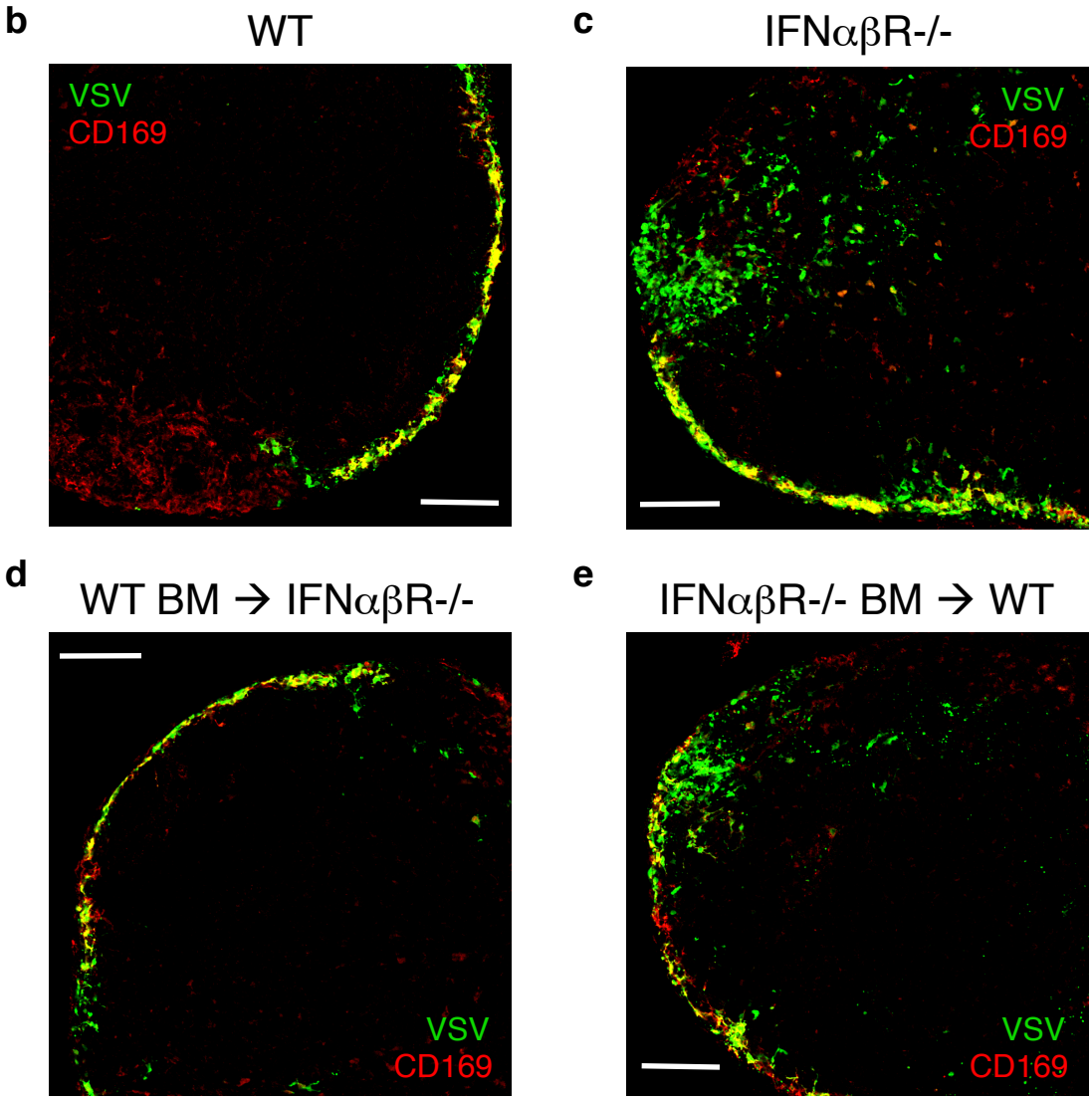
b
WT
VSV
CD169
c
IFNαβR-/-
VSV
CD169
d
WT BM → IFNαβR-/-
VSV
CD169
e
IFNαβR-/- BM → WT
VSV
CD169

Supplementary Figure 13. *Effect of hematopoietic or stromal IFNabR deficiency on survival and viral replication*. **a**, Kaplan-Meier survival curves of wild-type (WT), IFNabR$^{-/-}$ mice or irradiated wild-type mice that have been reconstituted with IFNabR$^{-/-}$ bone marrow (IFNabR$^{-/-}$ BM→ WT) that have been treated (or not) with CLL prior to challenge with VSV in the footpad. n = 8; WT + CLL versus IFNabR$^{-/-}$ BM → WT, P < 0.0001; IFNabR$^{-/-}$ versus IFNabR$^{-/-}$ BM → WT, P = 0.0002; Log-rank (Mantel-Cox) test. **b-e**, Confocal micrographs of footpad VSV-eGFP (green)-infected popliteal LNs from WT (**b**), IFNabR$^{-/-}$ (**c**), WT BM→ IFNabR$^{-/-}$ (**d**), IFNabR$^{-/-}$ BM→ WT (**e**) mice. Scale bars reflect 100 μm. Anti-CD169 (red) was used to stain LN macrophages. Micrographs are representative of 2 independent experiments that showed similar results.

Supplementary Movie Legends

Supplementary Movie 1. Three-dimensional rotation view followed by Z-stack projection of the MP-IVM stack used to generate Fig. 2e. The z-stack consists of 84 optical sections (z-increments of 1 mm) at a pixel density of 1024x1024. The popliteal LN from a VSV-eGFP-infected macrophage-sufficient mouse was stained with b3-tubulin (red) to label peripheral nerves. Blue signal denotes second harmonic signal from collagen in the LN capsule.

Supplementary Movie 2. Three-dimensional rotation view followed by Z-stack projection of the MP-IVM stack used to generate Fig. 2f. The z-stack consists of 22 optical sections (z-increments of 1 mm) at a pixel density of 1024x1024. The popliteal LN from a VSV-eGFP-infected macrophage-depleted mouse was stained with b3-tubulin (red) to label peripheral nerves. Blue signal denotes second harmonic signal from collagen in the LN capsule.